DEVELOPMENT OF NANOSECOND PULSE DIELECTRIC BARRIER DISCHARGE PLASMA ACTUATORS TO CONTROL FLOW SEPARATION OVER AN AIRFOIL

UNDERGRADUATE HONORS THESIS

Presented in Partial Fulfillment of the Requirements for
Graduation with Distinction in the
Department of Mechanical and Aerospace Engineering at
The Ohio State University

by

Christopher James Wiet

Advisor: Dr. Mohammad Samimy

****

The Ohio State University
May 2012

ABSTRACT

Separation of flow from the surface of an airfoil is a great limiting factor in the development of aerodynamic capability. Many methods of controlling or eliminating separation have been explored, but a relatively new technique involves affecting the flow field with a plasma actuator adhered to the surface of the airfoil. Extensive research using a specific type of actuator that utilizes dielectric barrier discharge (DBD) has shown that separation of flow from an airfoil can be reduced or eliminated when forced at the proper frequency. Furthermore, a shift from an alternating current (AC) to a nanosecond (NS) pulsed system has demonstrated control authority at various post-stall angles of attack (α) for Reynolds numbers (Re) and Mach numbers (M) up to 1.15×10^6 and 0.26 respectively (free stream velocity, U_∞= 93 m/s). The control mechanism for the NS-DBD is a thermal perturbation that creates strong compression waves that radiate into the freestream flow, resulting in either an active trip of the boundary layer, or the generation of coherent spanwise vortices that transfer momentum to the separated region. Such actuators were incorporated into two feedback control systems. An on/off controller was successfully established, but an extremum-seeking algorithm demonstrated only sporadic effectiveness.

ACKNOWLEDGEMENTS

I would like to thank, first and foremost, my advisor Dr. Samimy. He has been not only willing to serve as a mentor and teacher, but has provided the entire GDTL with world-class facilities. I feel privileged to have been able to work in his lab the last few years. Furthermore, I would like to thank Jesse Little, Chris Rethmel and Ani Sinha, as they were the ones who not only showed me the inner workings of the lab, but taught me the correct way to conduct reputable research. Of more recent support has been Cameron DuBois, and I would like to thank him for being a great collaborator in my most recent work. Also, all the other members of the GDTL have provided much appreciated help, discussion and feedback. Finally, I would like to thank my family and friends for being so supportive during recent weeks. Even when things got too busy for me to see them regularly, they were always ready to help in any way they could.

TABLE OF CONTENTS

LIST OF FIGURES

CHAPTER 1 Introduction

Transonic airfoils are not designed to develop sufficient lift at low speed. To get enough lift for take-off and landing, therefore, designers use elements such as flaps. Flaps are heavy and complex, but enable the flow on the suction side to remain attached to the airfoil surface. An alternate separation control method, however, could replace these flaps and eliminate some the weight, thus saving fuel during time of ever-increasing energy and oil prices.

The problem at hand is separation. This occurs when the angle of attack of an airfoil is increased, past a critical point at which the flow begins to separate from the surface of the airfoil, illustrated in Figure 1.1.

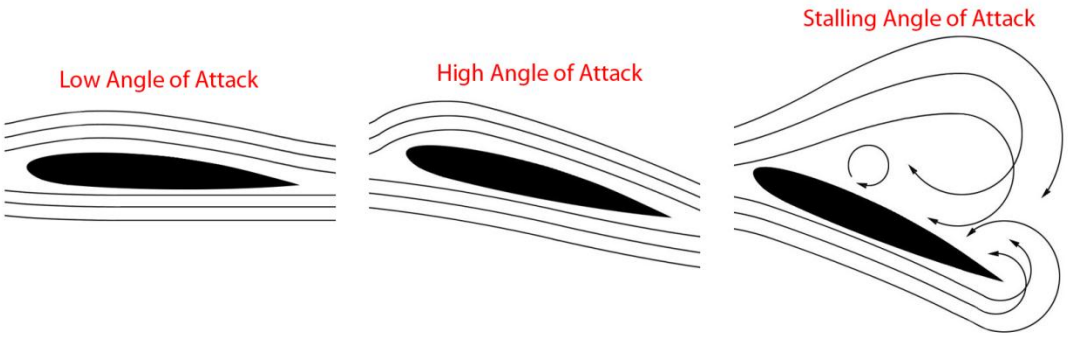

Figure 1.1: Effect of Increasing Airfoil Angle of Attack (Anonymous, Angle of Attack 2009)

When separation occurs lift is significantly reduced and drag is increased, eventually causing the airfoil to stall. This phenomenon is one of the greatest hindrances to the advancement of aerodynamic performance, and controlling or delaying its onset has interested engineering for nearly a century. Consequently, many methods of flow control have been developed to influence the separation location. The Gas Dynamics and Turbulence Lab (GDTL) at The Ohio State University is researching one of the newest separation control techniques which utilizes plasma actuators.

This thesis details the continued development of a nanosecond pulse driven dielectric barrier discharge plasma actuator (NS-DBD) to delay the onset of flow separation from an airfoil. It presents an overview of past projects at the GDTL and goes on to present the effectiveness of a NS-DBD on separation control on the leading edge of a NACA 0015 airfoil. Also presented are preliminary results of implementing such actuators into a feedback control system. Ongoing research is being conducted to characterize the turbulence levels in the wind tunnel facility used to test these actuators.

CHAPTER 2 Background

2.1 Introduction

In the study of separation control it is important to understand not only the physics of what causes separation, but how the flow behaves once separated. It is also beneficial to understand the history of different methods of separation control as well as common investigative techniques. A brief background in each of these areas is given here.

2.2 Airfoils

The reason airplanes can fly is purely a consequence of the shape of their wings. This shape is defined by a few universally standard parameters illustrated in Figure 2.1, below. The leading edge is the point at the front of the wing with minimum radius of curvature, while the trailing edge is the point of minimum radius curvature at the rear (Houghton, et al. 2013). The chord line is a straight line connecting the leading and trailing edges, and the chord length is the characteristic dimension of this shape and acts as the reference with which angle of attack is defined. The mean camber line is the locus of points midway between the upper and lower surfaces, and the thickness is either measured perpendicular to this line or the chord line.

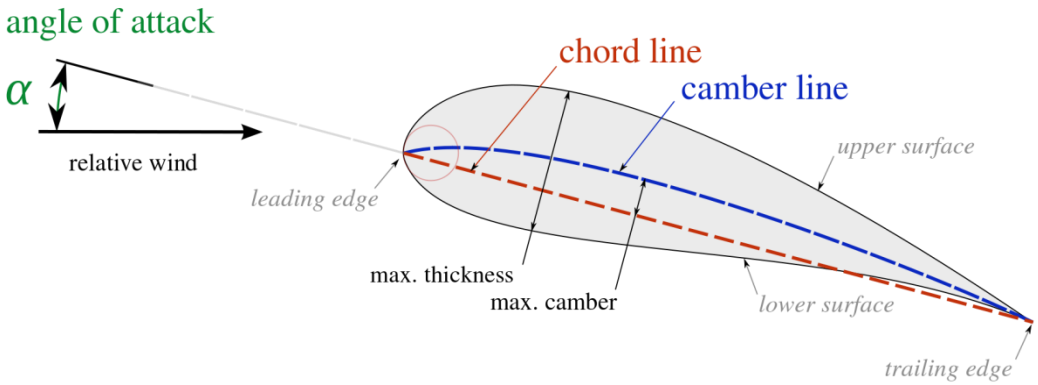

Figure 2.1: Airfoil Nomenclature (Anonymous, Airfoil 2012)

This shape, called an airfoil, is such that as fluid flows across its surface, a pressure difference is created between the top and bottom due to the difference in travel length of the fluid between these two surfaces. The law of conservation of energy dictates that, for a given stagnation temperature, the faster a fluid moves the lower its pressure. In the example of an airplane wing, therefore, since the air on the top has a greater distance to travel than that on the bottom in the same amount of time, the result will be low and high pressure regions on the top and bottom respectively. This pressure difference generates a net upward force called lift. The fact that air has momentum and is deflected by the airfoil, however, results another force called drag that opposes forward motion of the airfoil. The point at which drag begins to severely overtake lift is called the separation point.

2.3 Flow Separation

As stated above, separation is one of the most significant limiting factors on increasing the aerodynamic performance of airfoils. Flow separation occurs when an adverse pressure gradient causes the slow-moving fluid near the airfoil wall to detach from the surface (Greenblatt and Israel 2000), forming a region of stagnant or backwards-circulating fluid over the airfoil. In Figure 2.2, a sketch of the profile of the velocity, U, is shown at the point of separation. It indicates the result of a mathematical model of separation in a steady, two-dimensional flow. Note that not only is the velocity at the wall zero, which is always the case, but the gradient, $\partial U/\partial y$, is also zero.

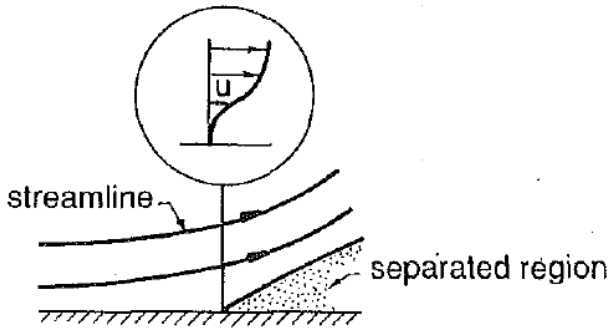

Figure 2.2: Diagram of Velocity Profile at the Point of Separation (Gad-el-Hak and Bushnell 1991)

Since flow characteristics are difficult to see in air, often times the flow is seeded with some form of particulate for better flow visualization. To better understand the result of separation, a smoke flow visualization experiment of the flow before and after separation is shown in Figure 2.3.

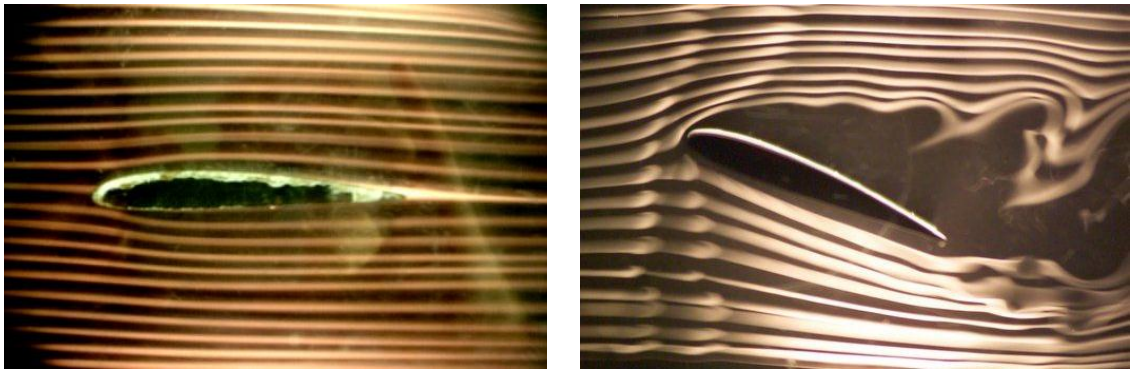

Figure 2.3: Smoke Flow Visualization of Attached (left) and Separated Flow (right) over an Airfoil (Devenport and Hartwell 2006)

In order to ensure that the experiments run on the scaled-down airfoil will translate effectively to full-sized wings, proper scaling techniques must be utilized. The most common scaling technique for separation control is to define non-dimensionalized quantities based on the separation length. Since this work involves leading edge separation control, the separation length is assumed to be the entire length, or chord, of the airfoil. One quantity central to this research is a non-dimensionalized universal parameter called the Reynolds number (Re). As shown in Equation (2.1), it is defined as the freestream velocity, U_∞, times the chord length, c, over the kinematic viscosity of the fluid, ν.

$$Re = \frac{U_\infty c}{\nu} \tag{2.1}$$

This quantity is used to compare our experiments with results in the literature describing Re at take-off and landing. This is necessary, as control of separation is futile if it cannot be obtained at Reynolds numbers at which flight takes place.

2.4 Passive Flow Control

Most methods of separation control in use today employ passive techniques, meaning control is achieved via physical modifications to the surface of the airfoil. Such elements include vortex generators, slotted flaps and slats, and their main purpose is to either divert the flow gradually or to force the flow to develop coherent periodic structures that act to use energy or momentum from the freestream to keep the boundary layer attached to the surface of the airfoil.

One of the simplest forms of passive control is the addition of flaps to the trailing edge of the wing. These flaps can change the effective chord or camber line of the airfoil, thus allowing it to change its lift/drag properties depending on the situation. Flaps, however, must be controlled by some form of mechanical drive or actuator. This adds a significant weight penalty and additional mechanical complexity.

Another form of passive control is via slats near the leading or trailing edge of the airfoil. The function of slats is to transfer momentum from the pressure (lower) side of the wing to the suction (upper) side. In doing so, the slow-moving air that makes up the boundary layer on the suction side is "energized", meaning it is given enough momentum to remain small and close to the airfoil surface. The cost of this momentum transfer, however, is a loss of lift due to a resulting change in pressure difference between the pressure and suction sides.

In the case of vortex generators, small plates are mounted to the surface of an airfoil so as to create a tip vortex which draws energetic, rapidly-moving air from outside the slow-moving boundary layer into contact with the aircraft skin. A secondary effect is known as "tripping" of the flow, as it causes the boundary layer to artificially transition from being laminar to turbulent. This is beneficial because turbulent boundary layers are known to increase the threshold of where separation occurs. The cost of installing these vortex generators, however, is added drag and weight.

Despite their drawbacks, these forms of passive separation control are effective when the airplane is operating under the specified design envelope. In fact, most aircraft in service today utilize some form of passive flow control. When in off-design conditions, however, these permanent modifications to the structure of the wing cannot be disengaged. This results in parasitic drag being incurred under some conditions when the passive control is ineffective. Because of this limitation, much effort has been put into developing new active flow control techniques that can be engaged and disengaged dynamically, while adding minimal weight and mechanical complexity to the plane.

2.5 Active Flow Control

In a general sense, active flow control is defined as adding energy directly to the fluid flowing past a surface (Gad-el-Hak and Bushnell 1991). This means control is achieved, not by redirecting the flow with a physical surface as in passive control, but by adding either momentum or a wave-carried excitation that "energizes" the natural flow instabilities. The main benefit of this type of control is that it is not permanent and may be disengaged during off-design conditions, effectively eliminating the parasitic drag experienced by passive control elements. In addition, some active control methods, such as plasma actuators, include little, if any, mechanical components. This, in turn, significantly reduced the mechanical complexity, and therefore weight, of the wing.

One of the first attempts at active flow control was direct tangential air injection via wall jets. This involves injecting high-pressure air upstream of the separation location to generate vortices that, much like passive vortex generators, delay separation. This is a very straightforward and therefore preferred flow separation control technique that has already been applied to military fighters currently in service (Gad-el-Hak and Bushnell 1991). A similar technique involves a "synthetic" air jet that utilizes a vibrating membrane instead of a high-pressure source and ducting to produce a pulse of air that interacts with the oncoming flow. Other flow control techniques involve acoustic excitation or, the emphasis of this research, plasma actuators.

While many of these active separation control techniques are still the subject of ongoing research, the most recent development is in the utilization of plasma actuators. Whereas air jets involve a mechanical component and/or extensive ducting, plasma actuators are purely electrical and take up little space or weight. Plasma, in general, describes the state that exists when electrical bonds in a gas are broken, creating free-standing electrons and ions that have been stripped from atomic nuclei. By applying a potential difference, or voltage, which is strong enough to generate stresses that drive a material to electrical breakdown, this phenomenon is brought about. This electrical activity initiates a stage of avalanching ionization, which eventually allows electrons to flow freely in space.

In an initial attempt to emulate the effect of air jets, a type of plasma created by a method known as dielectric barrier discharge (DBD) was investigated. In such actuators, an alternating current (AC) is sent to two electrodes that are separated by a dielectric material. When this is done, the atomic bonds in the air on the surface above the covered (ground) electrode are destroyed, thus creating free-flowing electrons, otherwise known as plasma. Similar to the blowing effects of air jets, AC-DBDs create an "ion wind" effect that adds momentum to flow, shown in Figure 2.4, below.

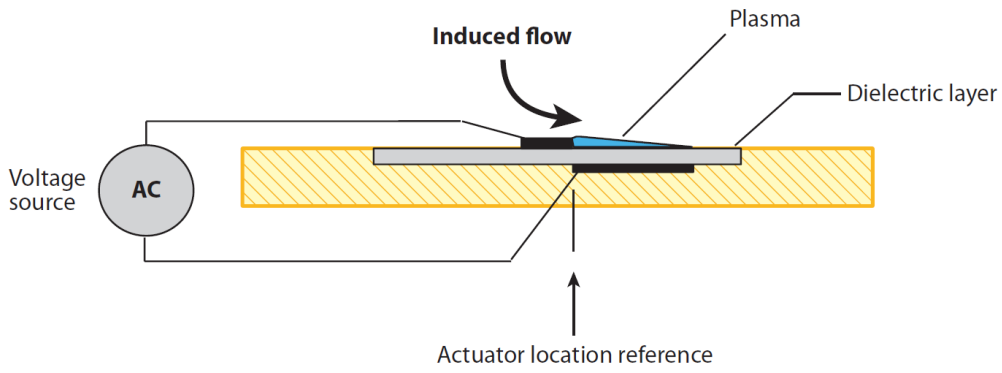

Figure 2.4: Diagram of DBD Plasma Actuator (Corke, Enloe and Wilkinson 2010)

Previous studies have shown AC-DBDs are capable of producing near wall jets with maximum mean velocities of ~3.5 m/s approximately 1 mm from the surface (Little 2010). This added momentum can result in one of two outcomes. The first is boundary layer tripping, and the second is energizing or

amplification of natural flow instabilities. The problem experienced with these actuators, however, is that the limited mean velocity generation allows for effectiveness only well under typical flight velocities. A different type of plasma actuator, therefore, is being investigated that utilizes a much faster pulse, known as a nanosecond pulse (NS) DBD (Roupassov, et al. 2009).

NS-DBDs are constructed exactly the same as AC-DBDs, but they operate on a timescale of about 50 ns, whereas AC-DBDs pulse with a period on the order of 400 μs. This means control is achieved in each type of actuator by fundamentally different methods. Since NS-DBDs operate at frequencies significantly above any frequencies present in the freestream flow, momentum addition similar to air jets or the AC-DBD is found to be ineffective (Little 2010). The pulse of an NS-DBD, however, creates extremely rapid localized heating at the interface between the two electrodes, so the control method is inferred to be a thermal phenomenon. The exact physics of the interaction are not fully understood, but it is known that the rapid localized heating generates compression waves that propagate into the flow (Little 2010), which are discussed in more detail in Section 4.3. These compression waves then act as a perturbation that, when forced at the correct frequency, generate coherent spanwise vortices that transfer momentum from the freestream to the separated region, thus reattaching the flow. The result is control authority that outperforms the control demonstrated by AC-DBDs (Rethmel, et al. 2011). For this reason, NS-DBDs are the exclusive topic of this research. A photograph of a DBD plasma discharge (purple glow) described above is shown in Figure 2.5.

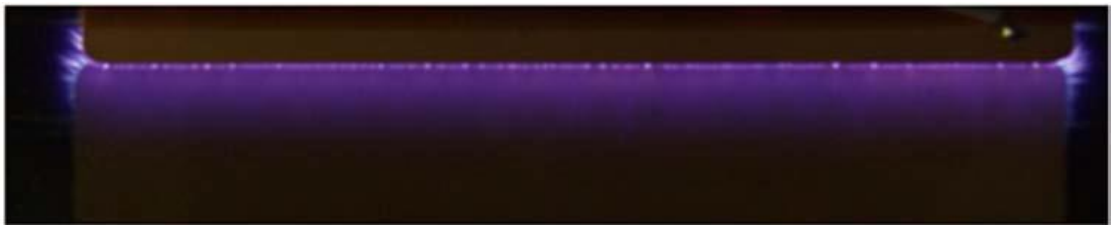

Figure 2.5: Photograph of an Active DBD Plasma Actuator

CHAPTER 3 Experimental Facility and Methods

3.1 Experimental Facility

The main testing facility for airfoil separation control at the OSU GDTL is a Göttingten-type recirculating wind tunnel. Air flow in the tunnel is created by an axial fan powered with a 200-hp variable speed AC induction motor. The fan speed is set using an operator keypad on the tunnel outfield just downstream of the test section. The tunnel also includes a built-in heat exchanger upstream of the nozzle contraction and a thermocouple just downstream of the test section to help maintain appropriate temperatures during testing. The heat exchanging mechanism has an automatic controller that adjusts the flowrate of coolant to keep the temperature inside the tunnel constant, even under different wind speed. For the purposes of this experiment, the controller was disengaged and the valve was set to fully open for every run. To ensure the airflow remains laminar throughout the tunnel, turning vanes are installed in each corner. A diagram of the wind tunnel construction is given in Figure 3.1.

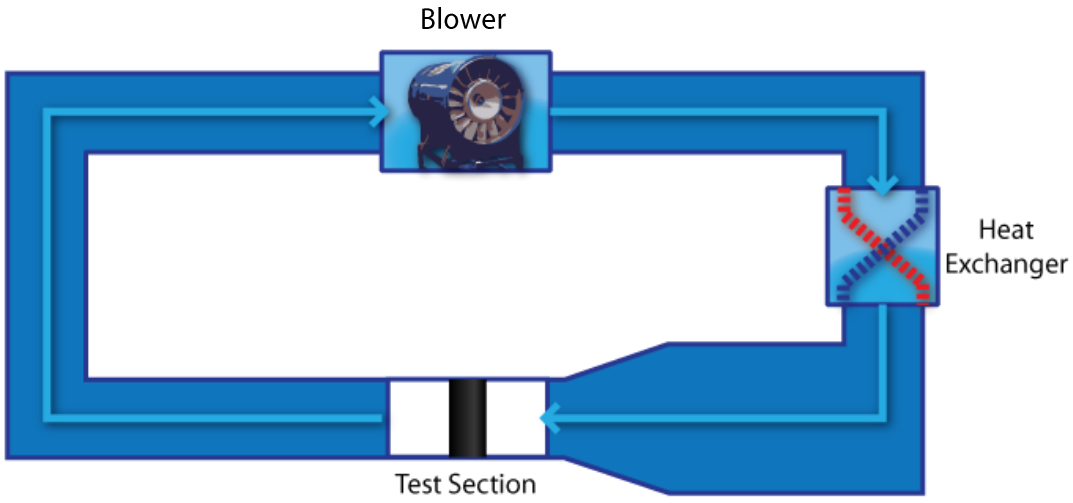

Figure 3.1: Diagram of Recirculating Wind Tunnel

The tunnel test section is $2\times2\times4$ ft^3 and is constructed of clear super abrasion resistant acrylic walls that are 1 inch thick, with one side able to be opened via heavy-duty hinges. The side-walls of the test section include 12-in diameter circular ports with removable disc covers (Figure 3.2). These are used both as a mount for the airfoil as well as an avenue for sensor lead wires and static pressure tubes to exit the test section without disturbing the flow inside the tunnel. They are held in place by three thumbscrews on either side and can be manually adjusted to change the angle of attack of the airfoil. The original system in place to set angle of attack was a protractor to measure angle and thumbscrews to secure the position of the airfoil. Recently, however, a digital angle indicator was installed to enhance both the accuracy and repeatability of this process.

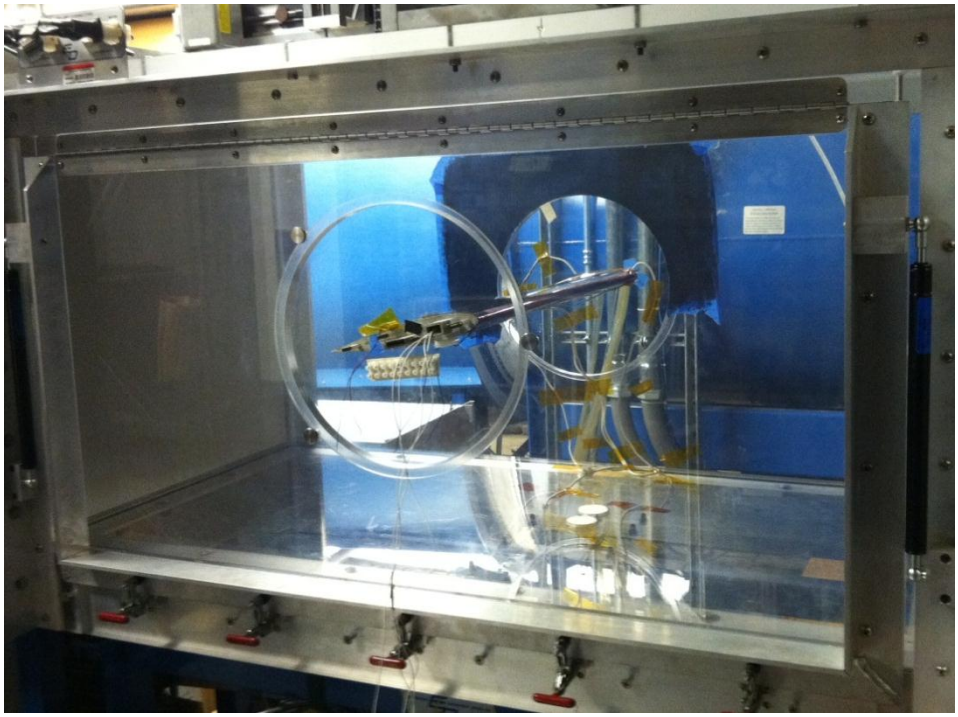

Figure 3.2: Test Section with Wall Plugs and Airfoil in Place

Figure 3.3: Instrument Panel for the Subsonic Recirculating Wind Tunnel

To characterize the freestream flow in the tunnel during a given test, two sets of differential static pressure transducers (Omega Engineering, Inc. PX655-25DI and PX655-5DI) are used to measure static (P) and dynamic pressure (q), while three process meters (Omega Engineering, Inc. DP-25-E-A) display the output in inches of water. The signals, in turn, are then routed to a data acquisition board (National Instruments PCI-6143), where a custom LabVIEW virtual instrument (.vi) is used to set the tunnel test conditions using Equation (3.1). Also input into this .vi are atmospheric pressure, relative humidity and tunnel temperature manually read from the instrument panel, shown above in Figure 3.3.

$$U = \sqrt{\frac{2q}{\rho}} \tag{3.1}$$

Where U is the flow velocity inside the tunnel (m/s), q is dynamic pressure (Pa) and ρ is the fluid density (kg/m^3). A pitot tube measurement was initially taken to prove the accuracy of the system and manual manometers are placed near the digital scales to confirm continued functionality.

A two axis traversing assembly (Velmex, Inc. Unislide) driven by a DC stepper motor and controller is mounted on top of the test section allowing introduction of instrumentation such as pitot tubes and hot wire probes through a 42.8-in long high density nylon brush seal along the tunnel ceiling centerline. To extend the reach of the traversing assembly into the tunnel, an aluminum support was fabricated and is shown in Figure 3.4.

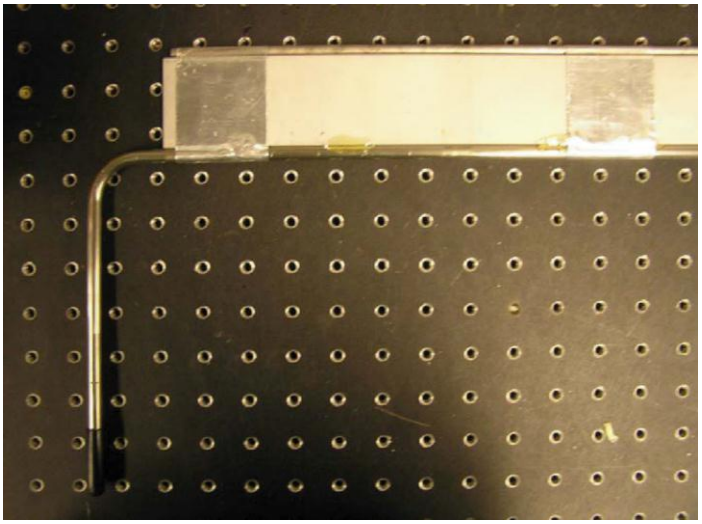

Figure 3.4: Modified Probe Extension Arm

Integrated into the current airfoil are three different sensing methods: 1) Static pressure taps, 2) Kulite pressure transducers, and 3) Hot-film sensors. The static pressure taps are located near the airfoil centerline entirely along its suction and pressure sides in the streamwise direction. Each tap has a 0.040-in diameter and all are acquired using three Scanivalve digital pressure sensor arrays (Figure 3.5).

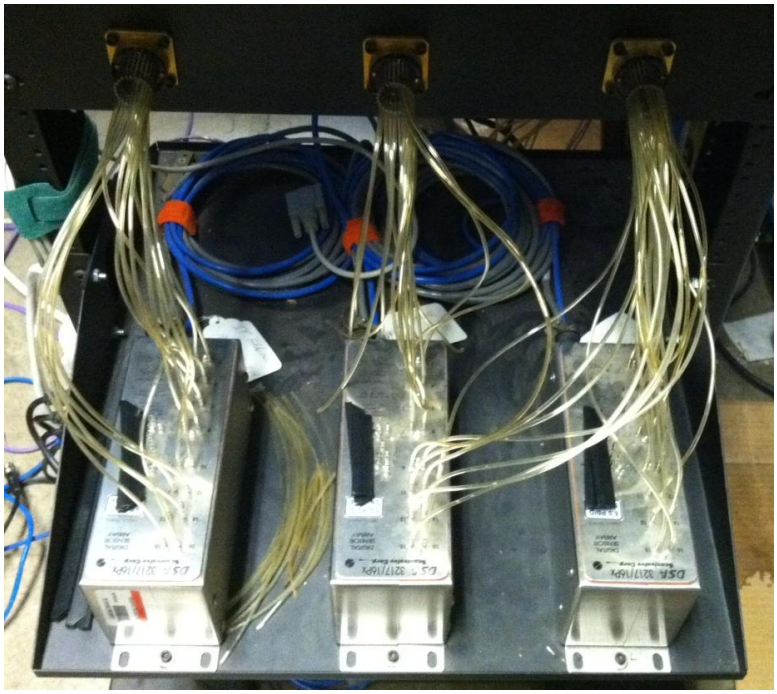

Figure 3.5: Scanivalve Pressure Sensor Arrays

Pressure data is averaged over 50 samples acquired at 10 Hz and used to calculate sectional lift coefficient, C_L, using numerical integration outlined in Equations (3.2) and (3.3).

$$C_P = \frac{p - p_\infty}{q_\infty} \tag{3.2}$$

$$C_L \approx \int_0^1 \left(C_{P,pressure\ side} - C_{P,suction\ side}\right) d(^x/_c) \tag{3.3}$$

Where p is the static pressure on the surface, p_∞ is the freestream static pressure, q_∞ is the freestream dynamic pressure and x/c is the chordwise position.

Two additional sensor types used are Kulite pressure transducers and Senflex® multi-element surface hot film sensors. Six Kulites are flush mounted with the airfoil surface and are used to characterize the pressure fluctuations within the tunnel. Average spectra are calculated from 32 blocks of 8192 samples which results in a frequency resolution of approximately 6 Hz. Two hot-film arrays are adhered to the surface of the airfoil, one from 37% to 63% chord length on the suction side and the other

from 11% to 17% chord length on the pressure side. Initially a four-channel constant-voltage anemometer (Tao Systems, Inc.) provided the necessary excitation. Currently, however, the hot films are run using a more typical constant temperature anemometer (CTA). These devices respond to changes in the shear stress on the surface of the airfoil, thus providing a fast approximation of the lift generated by the airfoil. These were used primarily for the purpose integrating the NS-DBD plasma actuator into a feedback control system, detailed in Section 4.4. The locations of all three sensing arrays are shown in the schematic in Figure 3.6, as well as the photograph in Figure 3.7.

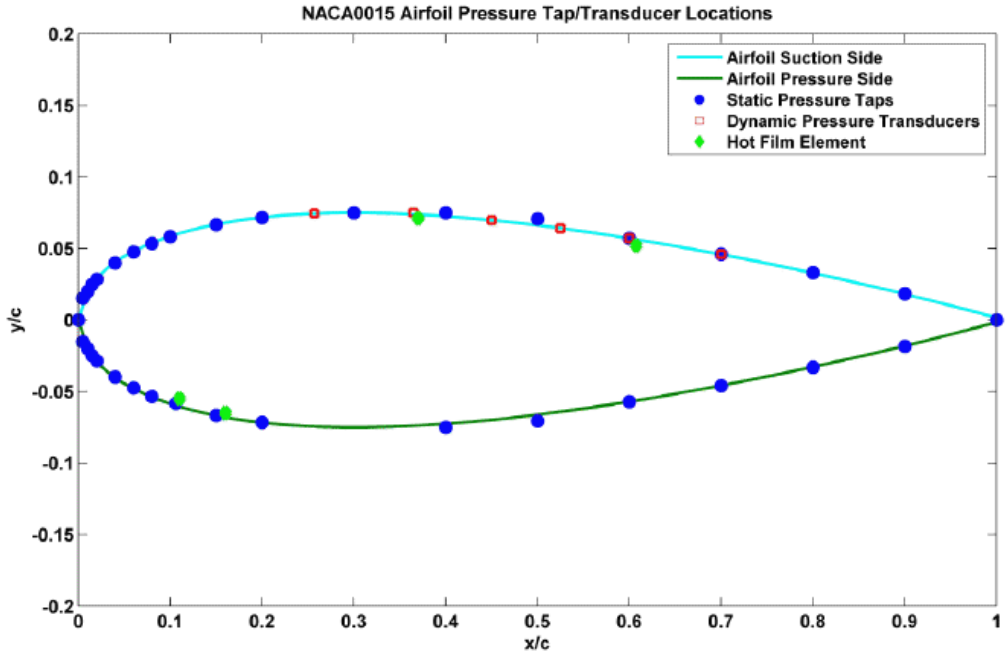

Figure 3.6: Instrumented Airfoil Schematic

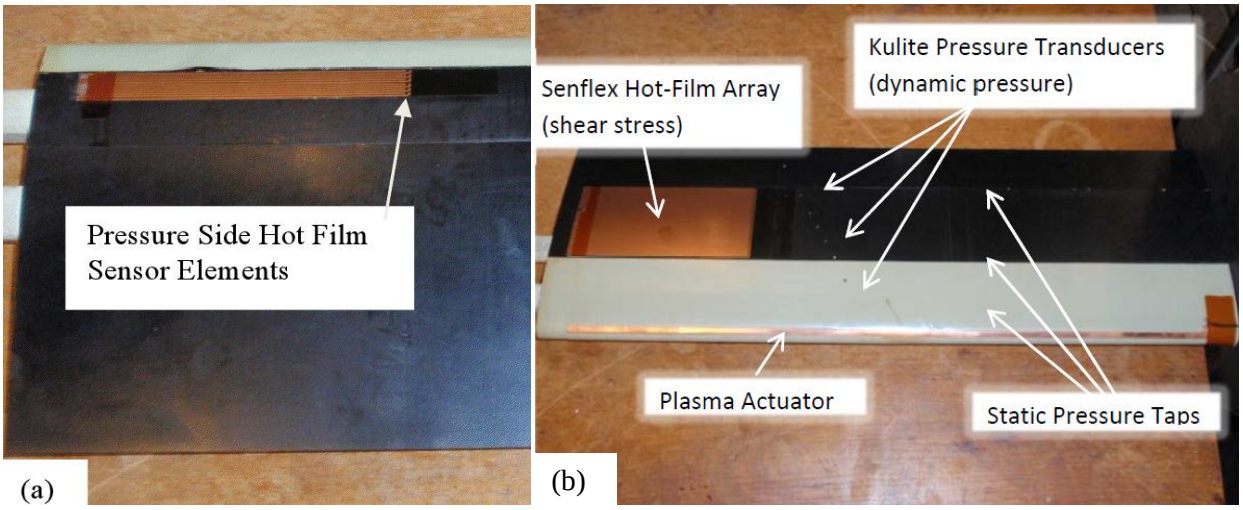

Figure 3.7: Sensors Installed on the (a) Pressure Side and (b) Suction Side of the Airfoil

3.2 NACA 0015 Airfoil

The airfoil currently undergoing testing at the GDTL facility is a NACA 0015 symmetric airfoil with an 8 inch chord and 12 inch span. As the name denotes, this airfoil profile was developed and characterized by the National Advisory Committee for Aeronautics (NACA) as part of a large group of related airfoils. The purpose of the project was to provide data that may be directly employed for a rational choice of the most suitable airfoil section for a given application (Jacobs, Ward and Pinkerton 1935). Since the purpose of this research is to examine and control separation effects only, the choice was made to utilize an airfoil with a simple profile that has been well documented in the literature. The NACA 0015 airfoil is symmetrical, the 00 indicating that it has no camber. The 15 indicates that the airfoil has a 15% thickness to chord length ratio. A schematic of the NACA 0015 profile is shown in Figure 3.6 above, with an illustration shown in Figure 3.9. Figure 3.8 presents the results of NACA Report No. 460.

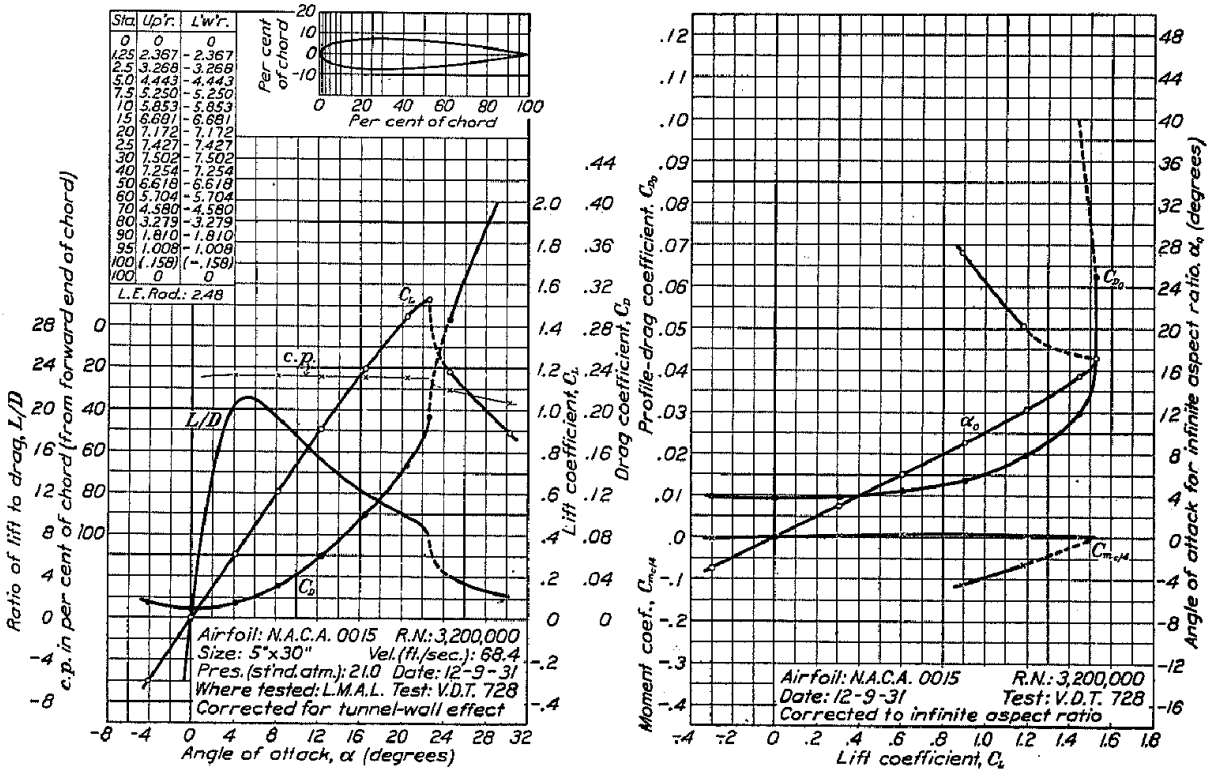

FIGURE 7.—N.A.C.A. 0015 airfoil.

Figure 3.8: NACA 0015 Airfoil Lift and Drag Curves (Jacobs, Ward and Pinkerton 1935)

In order to maintain the integrity of this profile when the actuator is installed, a 0.030-in recess has been cut along the leading edge of the airfoil extending from 10% chord length on the pressure side to 35% chord length on the suction side. This recess allows a DBD plasma actuator to be flush-mounted near the leading edge, while avoiding any significant discontinuities on the surface (Rethmel, et al. 2011). Also included in the construction of this airfoil is a modular design as shown in Figure 3.9. This not only allows access to the sensors mounted on the inside of the airfoil, but also provides the ability to interchange the recessed profile with a standard smooth profile.

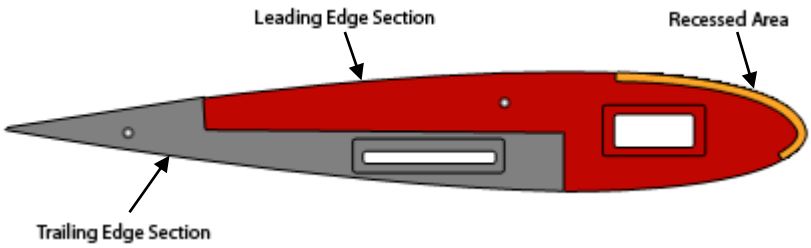

Figure 3.9: Illustration of Modular Airfoil Design

3.3 Nanosecond Pulse Dielectric Barrier Discharge Plasma Actuators

As previously described, the GDTL first investigated the effectiveness of a more traditional AC-DBD plasma actuator on separation control over the trailing edge of a high-lift airfoil. Of more recent interest, however, is the effectiveness of a NS-DBD plasma actuator on the leading edge of a simple, symmetric airfoil. The construction of the NS-DBD is identical to that of the AC-DBD. It is composed of copper tape electrodes separated by 3 layers of Kapton tape dielectric, totaling a 0.0105-in thickness.

The electronics system used to generate the pulse sent to the electrodes includes three basic elements (Figure 3.10 and Figure 3.11): a function generator, a high voltage power supply and an in-house built "pulser" that takes the input from the function generator and outputs the correct pulse to the electrodes on the airfoil. The power supply (Sorenson DCR 600-4.5B) is capable of supplying 650VDC, but is typically set to 600VDC in an attempt to extend the life of the actuator. The function generator (Tektronix AF6310) is simply used to send a square wave to the pulser, serving as a triggering mechanism. The specific waveform used is a $2.5V_{pp}$ square wave with a DC offset of 1.25V. The function generator is additionally set to burst mode with an external trigger so the frequency can be controlled by a computer via a dSpace rapid prototyping platform. The frequency is typically varied from 100 Hz to 1.5 kHz. In addition, a low voltage power supply is included to power dual cooling fans for the system.

Figure 3.10: NS-DBD High Voltage Power Supply

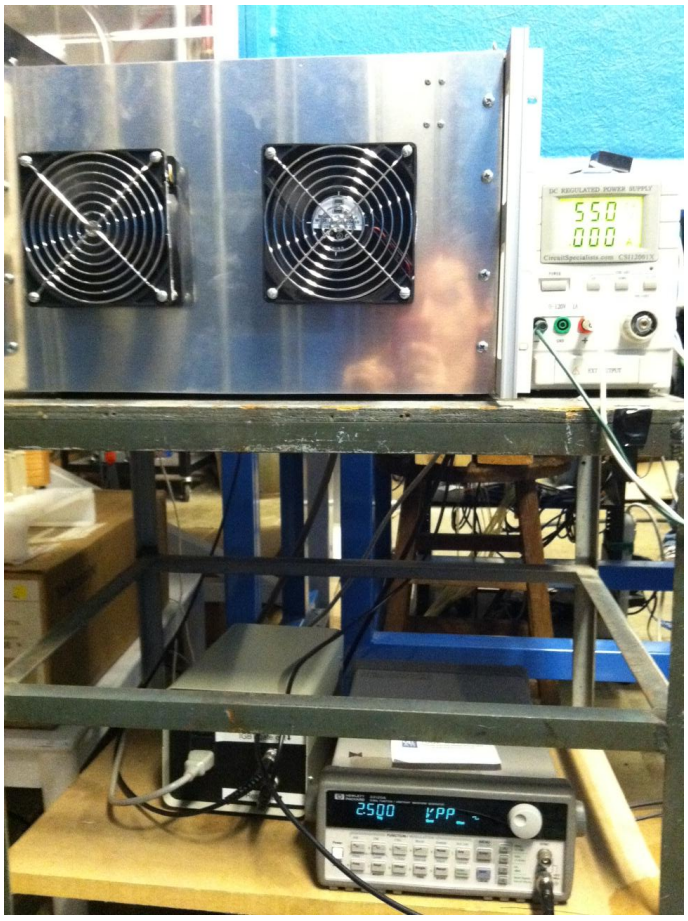

Figure 3.11: Picture of the Function Generator (bottom), Low Voltage Power Supply (top-right) and NS-DBD Pulser (top-left) Situated in the Infield of the Wind Tunnel

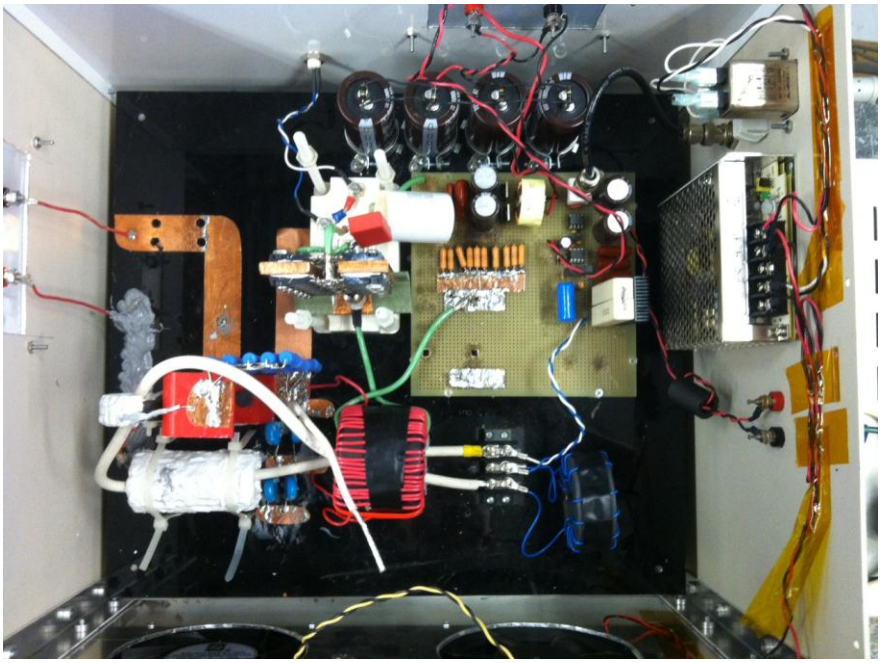

Figure 3.12: NS-DBD Electronics

The pulser, shown in Figure 3.12, was developed at OSU by the Nonequilibrium Thermodynamics Laboratory (NETL). The second generation model is currently being used for separation control experiments. The pulse voltage for the original pulser was ~15 kV for a test load of a ~30 cm electrode pair, while the peak current in discharge was 50 A. Peak power and energy was measured up to 600 kW and 17.5 mJ, respectively, but because of its very short time scale, its average power is less than the AC-DBD plasma actuator under similar operating conditions (Little 2010). Typical voltage, current, power and energy traces are shown in Figure 3.13.

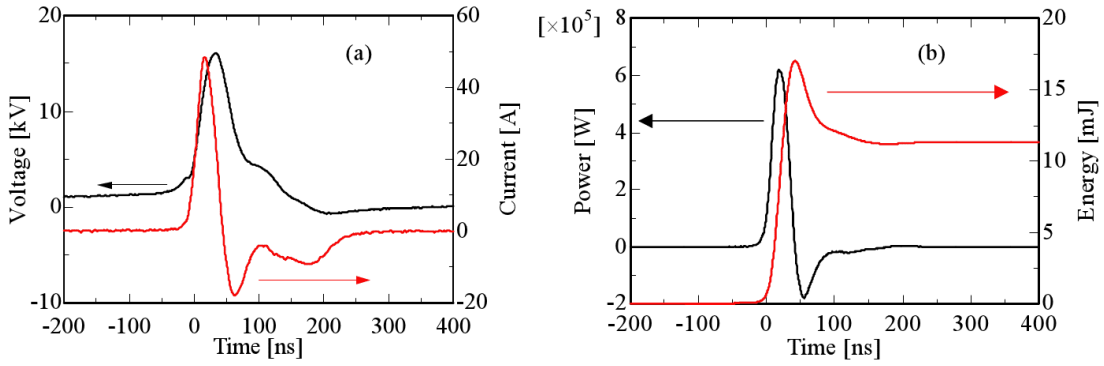

Figure 3.13: Typical Voltage, Current (a) and Power, Energy (b) Traces for an NS-DBD Plasma Actuator

This pulser showed leading edge separation control effectiveness at both high Re (1.15×10^6) and high α (18°) (Rethmel, et al. 2011). When experiments were run on a turbulent boundary simulated by a wall hump, however, no control effectiveness was demonstrated (Niekamp 2011). Since a turbulent boundary layer both exhibits a fuller velocity profile and extends further from the surface than its laminar counterpart, it is theorized that this is merely due to the fact that the plasma does not have enough power to leave the boundary layer and perturb the freestream flow. An effort, therefore, to increase the power generated by the pulser was undertaken by the NETL. The input for this new pulser is still ~15 kV, but the current produced is now ~100 A, resulting in a peak power and energy output of ~0.9 MW (50% increase) and ~50 mJ (180% increase) respectively, shown in Figure 3.14. This pulser was furthermore incorporated into a double actuator system, which is described in detail in Section **Error! Reference ource not found.**.

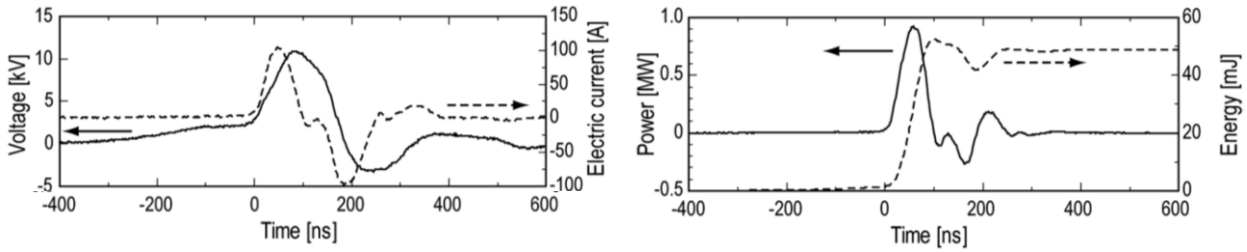

Figure 3.14: Time-Resolved Pulse Voltage and Current (top), Instantaneous Power and Coupled Energy (bottom) in a 148-cm long DBD Plasma Actuator (Takashima, et al. 2011).

CHAPTER 4 Results

4.1 Introduction

As described above, all tests were run in a recirculating wind tunnel at the OSU GDTL on a NACA 0015 airfoil. Static pressure taps on the airfoil were used to determine true lift during post processing, while hot films were used as an approximate gage of lift to be incorporated into a real-time feedback control system. Discussion below includes two baseline cases, the first having been performed before any experiments were run on the airfoil while the second is currently under investigation. After the first baseline flow characterization, experiments were conducted to investigate the open-loop control authority of the NS-DBD actuator. This was then expanded to include their use in both a closed-loop feedback control system as well as a multiple actuator setup. The following section presents the results of these studies.

4.2 Baseline Results

The first step in any experiment is to characterize a control or baseline case. As stated above, the GDTL NACA 0015 airfoil has an 8-in chord length and 12-in span, and baseline characteristics were first determined using the leading edge module with no recess (Rethmel, et al. 2011). Pressure data from the static pressure taps is first averaged over an entire test period, as all tests are run under assumed steady state. Average C_P is then integrated to calculate C_L as a function of α, a common metric to display airfoil characteristics. The maximum lift coefficient, $C_{L,max}$ is demonstrated around 12° for all Re, although the magnitude of $C_{L,max}$ varies, as expected, with Re. The range of $C_{L,max}$ between all Re considered in 1.0-1.1, as seen in Figure 4.1, below. Comparing Figure 4.1 with previous literature results in Figure 4.2 shows not only a strong similarity between the onset of separation near α of 12°, but also similar magnitudes for $C_{L,max}$.

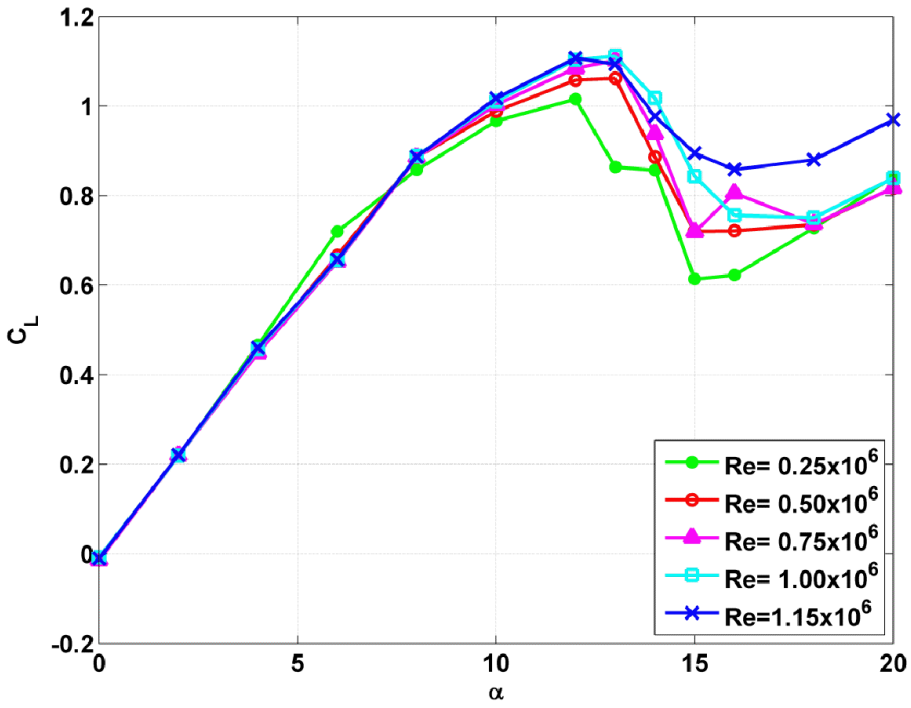

Figure 4.1: Lift Coefficient vs. Angle of Attack for Various Reynolds Numbers for the Baseline Case

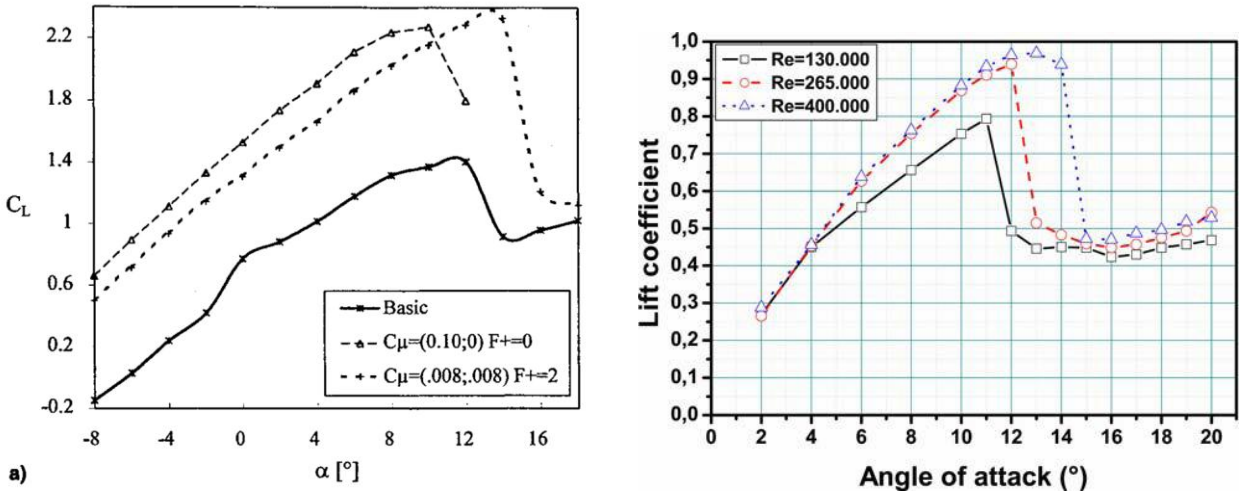

Figure 4.2: Plots of C_L vs. α for NACA 0015 Airfoil (Seifart, Darabi and Wygnanski 1996) (left) and (Benard, et al. 2010) (right)

4.3 Forced Results

With the above confirmation that the GDTL wind tunnel facility and airfoil were performing as expected, experiments were run testing the effectiveness of the NS-DBD plasma actuator on leading edge separation control. In an attempt to increase the precision and repeatability of the actuator, a method of creating the DBD electrodes via printed circuit board (PCB) techniques was investigated. Previous methods of DBD manufacture included not only laying copper and Kapton tape by hand, but also aligning the elements by sight. Commercially manufactured custom PCBs are quite costly, so a template (Figure 4.3) was constructed to facilitate an in-house etching process on readily available double-sided PCB material. The process includes first covering the blank PCB material with Kapton tape over the desired actuator location. Then the template is used to cut away excess tape, leaving only the desired actuator area left covered. Then the sheet is soaked in a bath of ferric chloride until all excess copper is removed from the sample. Once this process is complete, the sheet is washed off in tap water and the tape is removed. This allows the DBD actuators to be manufactured repeatibly and accurately.

Figure 4.3: PCB Template for Covered (upper) and Exposed (lower) Electrode

A comparison between the effects of actuation with the PCB actuator and the Kapton tape actuator for both low and high Re is shown in Figure 4.4, below. It can be observed that the PCB actuators demonstrate similar control authority to the already established Kapton tape actuators.

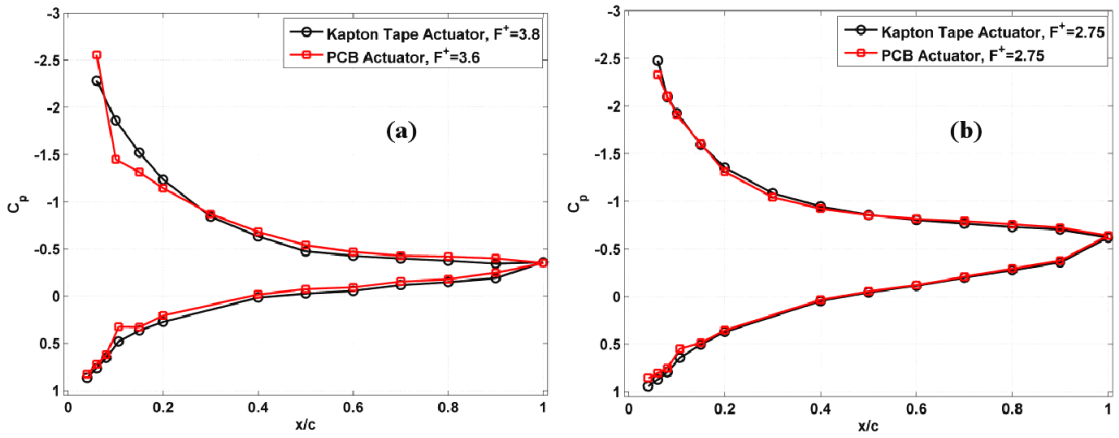

Figure 4.4: Controlled C_P Comparison for Airfoil with Kapton Tape Actuator and for Airfoil with PCB Actuator at (a) $Re = 0.25 \times 10^6, \alpha = 14°$, and (b) $Re = 1.15 \times 10^6, \alpha = 20°$

As introduced in Section 2.5, NS-DBDs are found to exhibit two main methods of flow control. In both cases, however, the perturbation is caused by Mach waves generated by the rapid localized heating at the electrode interface. Phase-locked schlieren imaging performed by (Takashima, et al. 2011) at the OSU NETL has visually captured these waves, shown in Figure 4.5 and Figure 4.6, below.

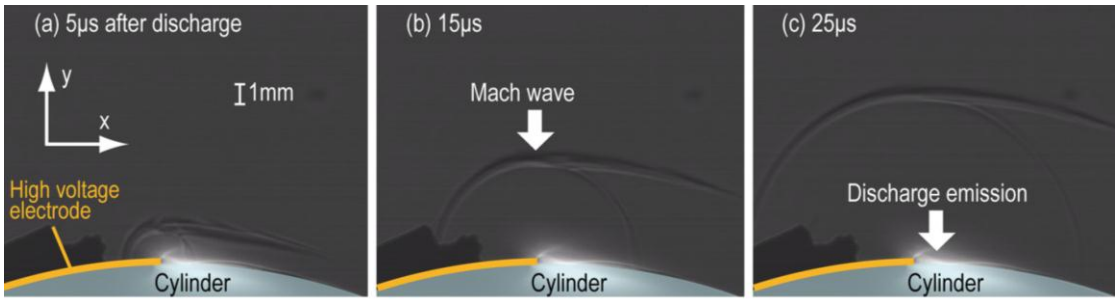

Figure 4.5: Schlieren Imaging of NS-DBD Compression Wave (Side View)

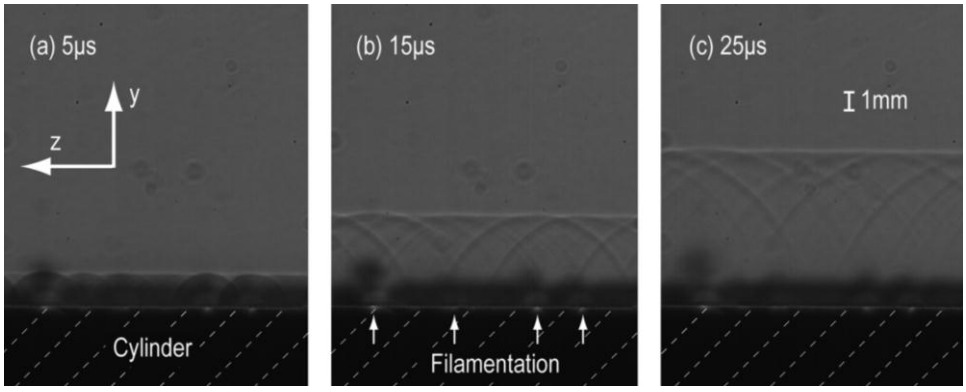

Figure 4.6: Schlieren Imaging of NS-DBD Compression Wave (Top View)

Considering both the side and top view shows that the result of the actuation is a compression wave that radiates in the general form of a cylinder from the interface of the covered and exposed electrodes. Certain plasma concentrations or "hot spots" are evident in these images, but after 25 μs they seem to combine into a line of effective perturbation.

By examining the effect of forcing frequency on control authority, a theory can be formed on the method of flow control. The frequency, in this case, is a non-dimensionalized frequency normalized by the airfoil chord length and freestream velocity defined as follows:

$$F^+ = \frac{fc}{U_\infty} \tag{4.1}$$

Examining Figure 4.7(a) shows the NS-DBD demonstrates significant control authority, but Figure 4.7(b) suggests that, because of the lack of preferred frequency, the actuators function as an active trip of the boundary layer. Examining Figure 4.8(a) shows a similar control authority of the NS-DBD at high Re and high α, but Figure 4.8(b) shows a clear preferred frequency around $F^+ = 1.9$. This is fairly consistent with dimensionless frequencies around $F^+ \approx 1$ observed in literature for effective instability excitation (Seifart, Darabi and Wygnanski 1996). The conclusion is that as Re is increased, the separation control method of NS-DBDs shifts fundamentally from an active trip of the boundary layer to an enhancement of the natural instabilities present in the flow over the airfoil (Rethmel, et al. 2011).

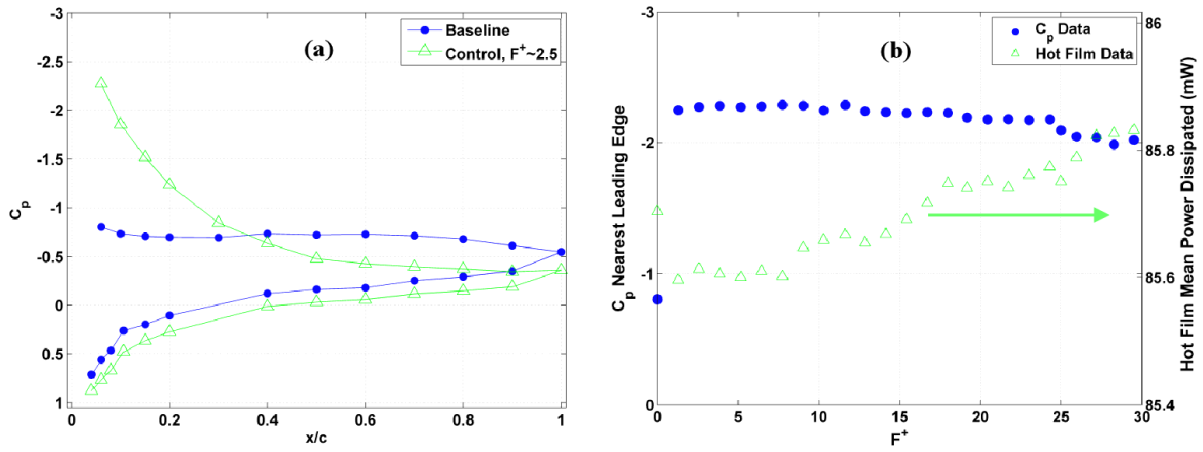

Figure 4.7: (a) C_P Curves Comparing Baseline and Control Cases ($F^+ = 2.5$), and (b) Hot Film Mean Dissipated Power and C_P Nearest Leading Edge for Various Forcing Frequencies, F^+, at $Re = 0.25 \times 10^6, \alpha = 14°$.

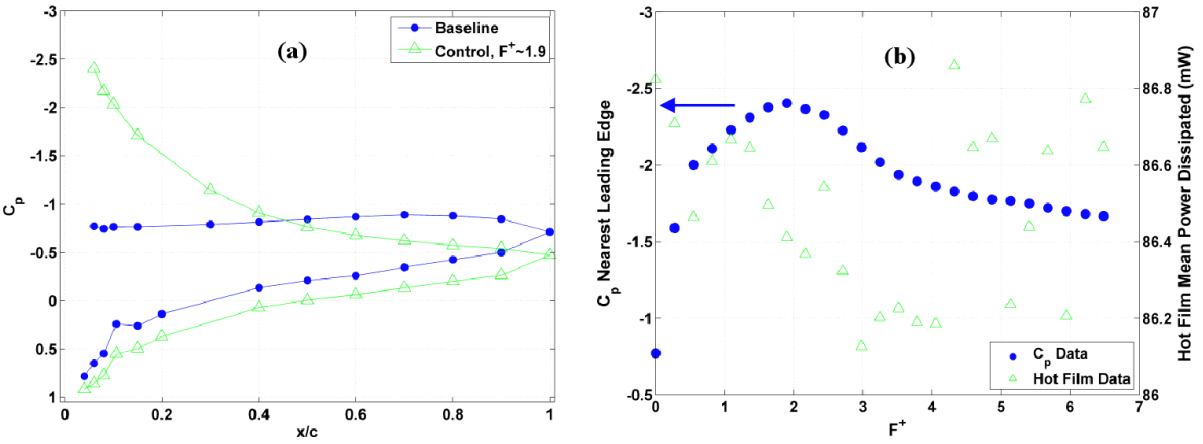

Figure 4.8: (a) C_P Curves Comparing Baseline and Control Cases ($F^+ = 1.9$), and (b) Hot Film Mean Dissipated Power and C_p Nearest Leading Edge for Various Forcing Frequencies, F^+, at $Re = 1.15 \times 10^6, \alpha = 18°$.

4.4 Feedback Control

Once control authority of the NS-DBD actuators was established, it was sought to incorporate them into a feedback control system. The most basic example of a feedback controller is to command a system to perform an action only when a sensor detects when one parameter has crossed some pre-determined threshold. This was the first step in the development of a feedback control system for separation control, known as on/off control. Since static pressure taps have a low frequency response and the dynamic pressure data gathered from the existing Kulite pressure transducers does not correlate well with lift, a surface-mounted hot film sensor was chosen as the feedback sensor. Since the hot film array

located on the pressure side of the airfoil is located closer to the leading edge than the suction side array, it was chosen as the target region for this study. Hot films provide of measure of the shear forces at the airfoil surface. For the hot films on the pressure side, therefore, the more lift the airfoil produces the lower the power dissipated. After some initial testing, it was found that the hot films dissipate about 88.5 mW when separated at $Re = 1.15 \times 10^6$ and a little less than 87.5 mW when attached, so a nominal threshold was chosen at 87.5 mW. In addition, a region surrounding the nominal threshold called a "dead zone" was defined so as to prevent rapid switch of the actuation state. In Figure 4.9, the hot film signal starts the run above the specified threshold while the actuator is turned off. Once the closed-loop control is turned on at $t = 1\ sec$, the control algorithm recognizes this and turns the actuator on. This causes the flow to become attached, thus lowering the power dissipated in the hot film. Since the hot film signal never falls below the dead zone, the actuator remains engaged throughout the entire run. In short, this effectively demonstrates a feedback control system with on/off capability for separation control utilizing NS-DBDs.

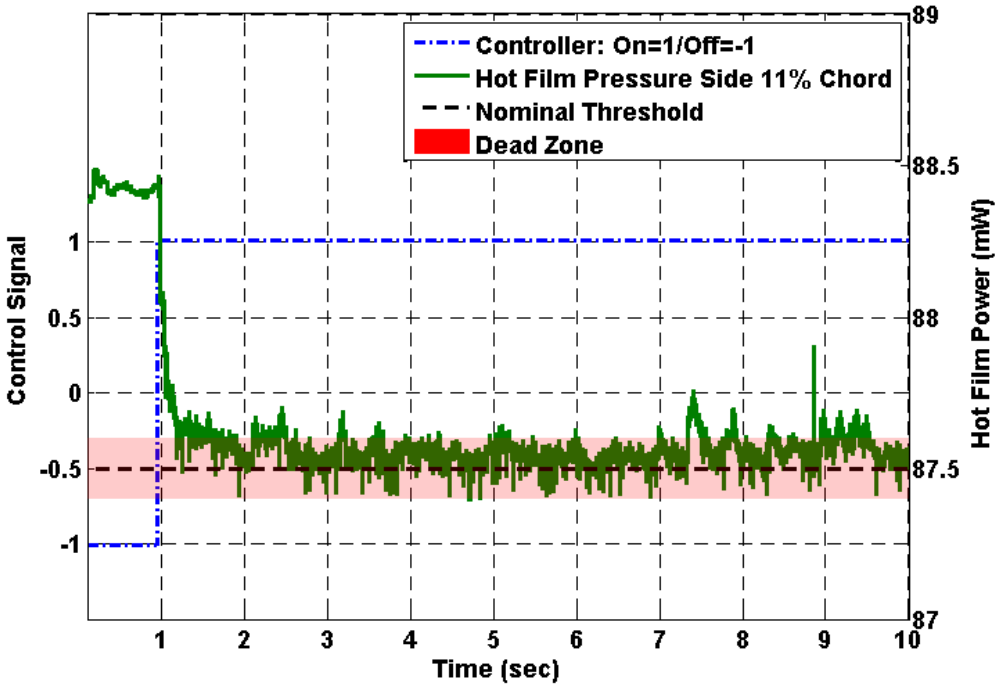

Figure 4.9: On/Off Controller at $Re = 1.15 \times 10^6, \alpha = 20°$

Once on/off control was firmly established, the next step was to attempt an extremum-seeking algorithm. As shown in Figure 4.8, at high Re the control authority of an NS-DBD depends greatly on actuation frequency. With this in mind, a method of dynamically varying the frequency and of automatically optimizing its effect was investigated. The algorithm chosen for this application is a Modified Nelder-Mead Algorithm, as its effectiveness was previously shown in high Reynolds number high-speed jet forced with localized are filament plasma actuators (Sinha, et al. 2012). A diagram of the logic employed by this algorithm is given in Figure 4.10.

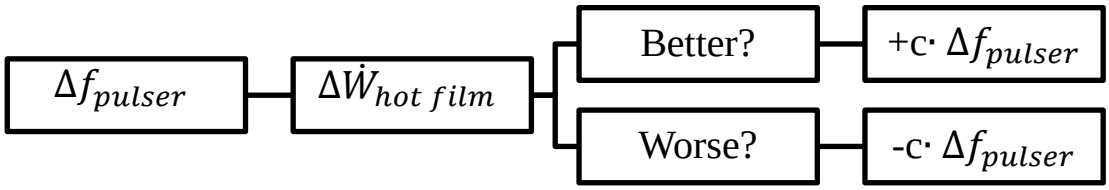

Figure 4.10: Modified Nelder-Mead Algorithm Logic Diagram

This algorithm can be described as follows: first the frequency of the actuator is changed by some value, after which the hot film power dissipation is analyzed. If the algorithm determines the result is better than the previous condition (i.e. power dissipation decreases) it changes the frequency again in the same direction. If, however, it decides the result is worse than the previous condition (i.e. power dissipation increases) it changes the frequency in the opposite direction. The result of this logic is a controller that automatically settles into a minimum value of the sensed parameter. The drawback, however, is that this algorithm cannot determine the difference between a local and global minimum, meaning it has a tendency to get "stuck" at suboptimal values. Results of preliminary tests for this algorithm are presented below.

The figures below represent two separate runs operating under the exact same experimental parameters. As is evidenced by the fact that each run resulted in different end results, it is apparent that the current extremum-seeking algorithm and sensor location setup are not very robust. This, however, is

not unexpected because of the known limitations of the algorithm described above. In the trials shown below, the velocity in the tunnel is varied from $Re = 0.25 \times 10^6$ to the maximum tunnel capability and then back down, all while the feedback controller is running. The trial shown in Figure 4.11 shows good actuator frequency optimization while the tunnel speed is increasing and while the tunnel is resting at its maximum velocity. Once the velocity is decreased, however, the algorithm attempts to converge on some local minimum not corresponding with the absolute minimum. The controller, in turn, cannot escape its current path and eventually diverges, resulting in a very high frequency corresponding to no control authority. The trial shown in Figure 4.12 shows similar effectiveness to the previous case during the period of increase in tunnel velocity. Once the tunnel velocity is decreased, however, it experiences a similar problem as the first case between 300 and 350 seconds, as evidenced by the spike in frequency and drop in C_P. In this case, though, the algorithm is able to climb out of the local minimum and continue until it reaches the global minimum around $F^+ = 1$.

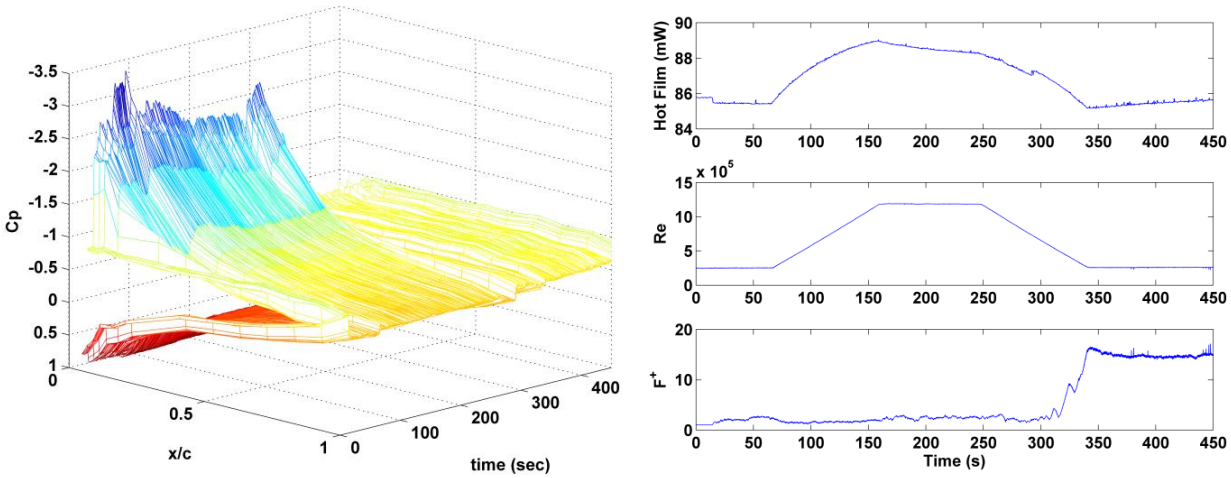

Figure 4.11: Extremum-Seeking Control: Re varied from 0.25×10^6 to 1.15×10^6 to 0.25×10^6, $\alpha = 18°$

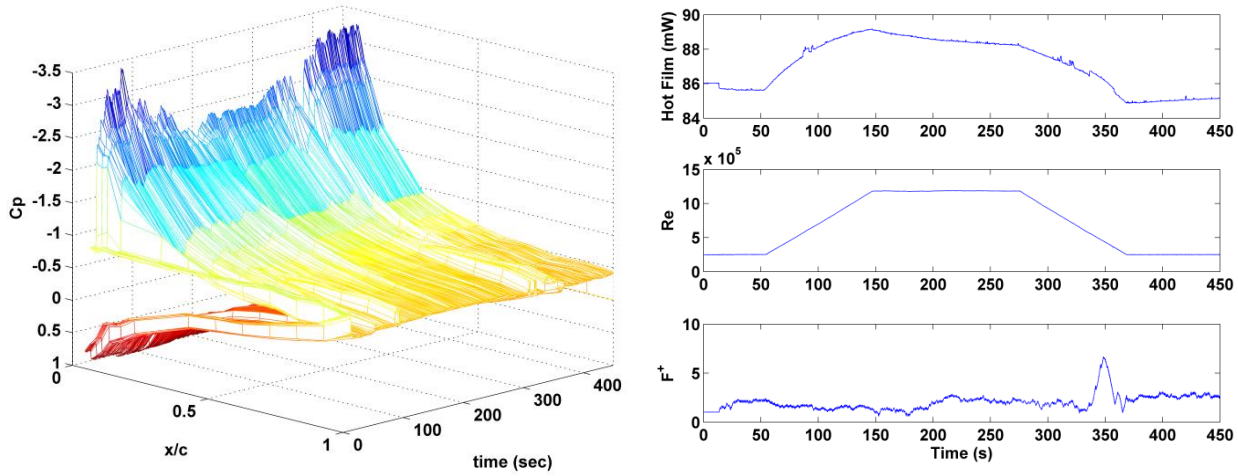

Figure 4.12: A Second Run of Extremum-Seeking Control Under the Same Parameters as Figure 4.11

Another factor in the instability of the feedback system is also due to the placement of the sensors. Since the current airfoil contains a recess, the hot film arrays were not attached very close to the stagnation point on the airfoil, meaning the gradient of pressure distribution is not at its maximum. Still, although this algorithm is not robust and the setup is not ideal, it is encouraging to see some results which indicate that more advanced feedback control may prove successful in this application.

4.5 Change in Baseline Behavior

During some recent experiments, it was seen that the baseline performance of the airfoil seems to have changed. The result of that baseline test is presented in Figure 4.13.

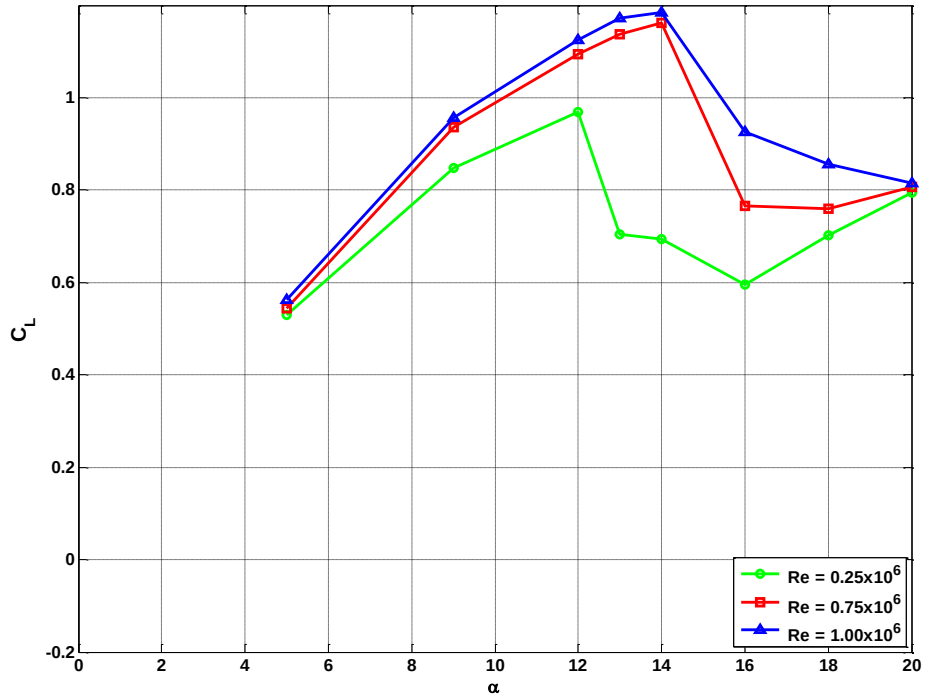

Figure 4.13: Second C_L vs. α Airfoil Baseline Characterization

When compared with the original baseline test (Figure 4.1), this shows fairly good correlation of airfoil performance at the slowest speed of $Re = 0.25 \times 10^6$. As the velocity is increased, however, C_L keeps increasing until it peaks, not at 12° as demonstrated previously, but at 14°. This means the flow over the airfoil appears to remain attached at greater angles of attack than are documented in literature, thus casting doubt on the suitability of the experimental rig as a test facility for examining the NS-DBD control authority. A conceivable cause for this extended attachment is high turbulence levels within the tunnel. Several non-averaged pressure curves tracked through time are presented in Figure 4.14 through Figure 4.16. Of note is that the C_P curves are not continuous at $x/c = 0$ because the presence of the actuator electrode prevented pressure measurements from being able to be taken.

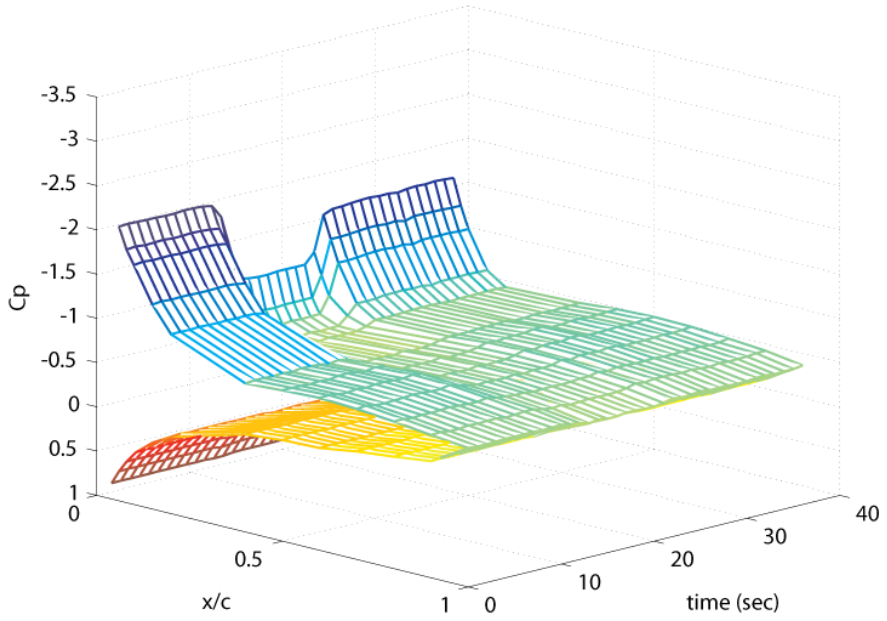

Figure 4.14: Unsteady Behavior of C_P vs. Chordwise Position, ($Re = 1.0 \times 10^6,\ \alpha = 13°$)

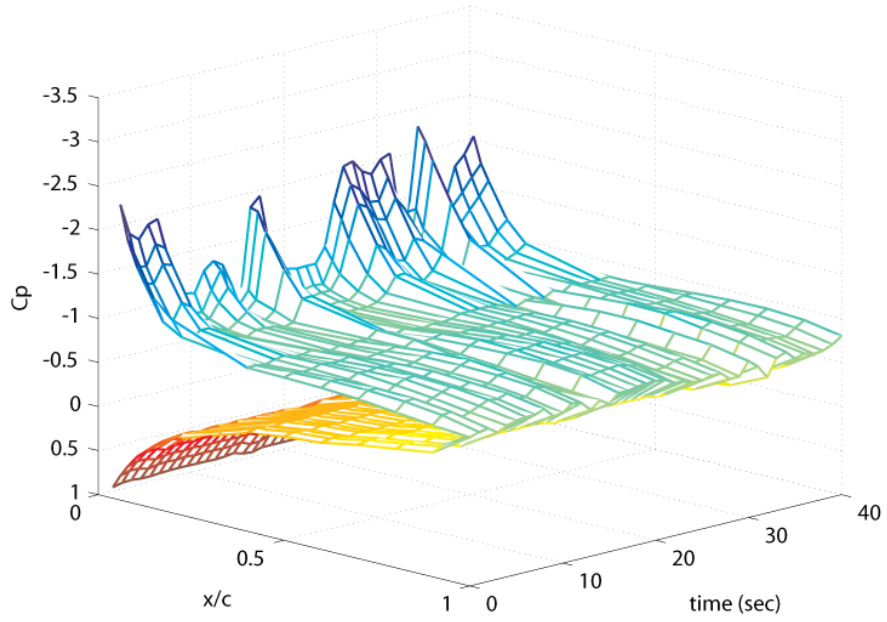

Figure 4.15: Additional Unsteady Behavior of C_P vs. Chordwise Position ($Re = 1.15 \times 10^6,\ \alpha = 16°$)

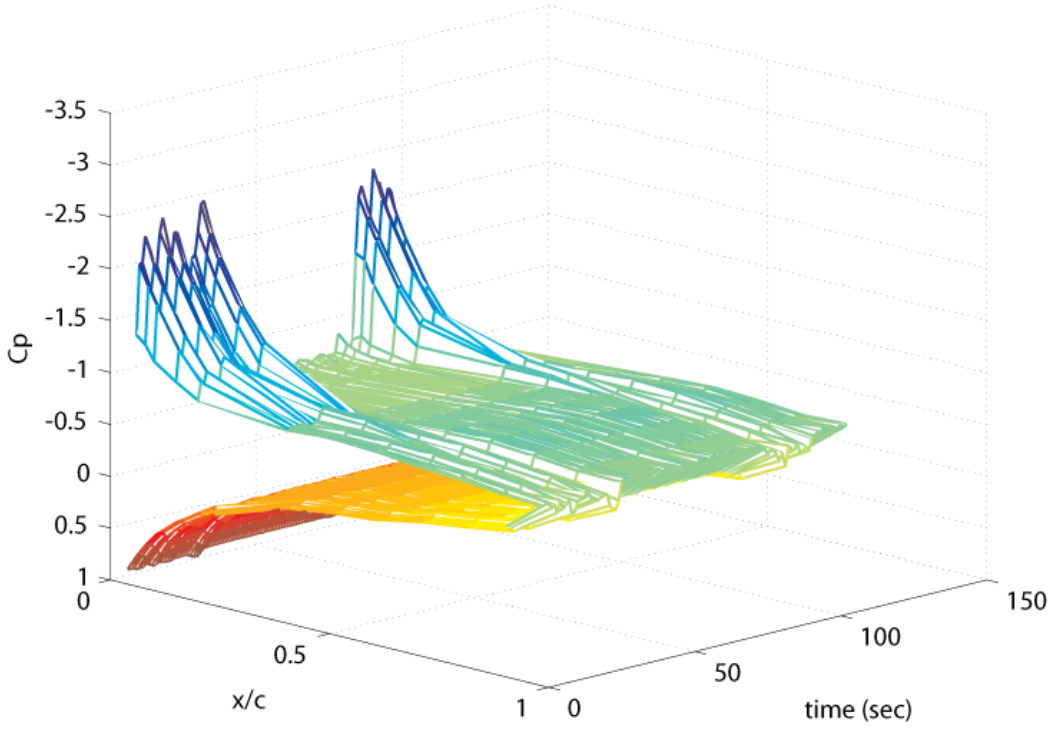

Figure 4.16: Unsteady Behavior of C_P vs. Chordwise Position Demonstrated Over Long Period ($Re = 1.15 \times 10^6$, $\alpha = 16°$)

Figure 4.14 shows a C_p curve at an angle of 13°, which is very near the expected separation angle. The flow clearly exhibits some form of transience as there is a noticeable drop in suction around 10s, which then rises again around 25s. Figure 4.15 then considers an angle of 16°, which is a case well within the expected region of separated baseline flow. In this case, the transience is much more random but multiple peaks and dips in suction are still evident throughout the run. To ensure this behavior is not simply a small transient phenomenon that eventually smooths with time, a similar run was performed for a longer period of time, presented in Figure 4.16. This shows significant peaks in suction around 10s and again around 100s with severely stalled sections in between. This further bolsters the presumption that some form of excessive turbulence is present in the tunnel, as a turbulent boundary layer is known to delay separation in an airfoil. To investigate this hypothesis, experiments are currently being performed to characterize the turbulence levels in the tunnel using a TSI 1210-20 hot-wire probe.

CHAPTER 5 Conclusions and Future Work

Separation is one of the largest obstacles in further enhancing the performance of airfoils. Various passive control techniques have been demonstrated to provide effective separation control, and many are already implemented into airplanes today. These techniques, however, produce inefficiencies such as increased drag and weight that severely outweigh the benefits when operating in off-design conditions. A new genre of separation control known as active flow control, therefore, is currently the subject of much current research. The goal of these active techniques is to achieve similar control authority to passive techniques, but then be able to be turned off when no longer needed or beneficial. Research at the OSU Gas Dynamics and Turbulence Laboratory has been investigating one such technique. It utilizes plasma actuators to perturb the oncoming flow, and, via various mechanisms, cause it to reattach to the surface of the airfoil. The type of plasma is called dielectric barrier discharge. Two variations of DBDs are currently under the most investigation with AC-DBDs being more firmly established and NS-DBDs being more up-and-coming. NS-DBDs operate under a much faster pulse than AC-DBDs and therefore affect the flow, not with blowing effects, but with thermally-induced compression waves. These waves provide a more powerful perturbation than that found in AC-DBDs, so separation control has been established all the way to 93 m/s and 18° angle of attack. After proving NS-DBDs could be effectively integrated into an on/off feedback control system, it was sought to optimize their effect via an extremum-seeking feedback system. The resulting controller was not very stable, but at least the door is open to further refinement. In addition, the GDTL facility was fitted with the capability to control a two-actuator setup. The state of each discharge point is able to be controlled independently, but the frequencies of both are linked, as their signals originate from a single pulser.

Further study is currently underway to characterize the turbulence levels within the tunnel itself. Once this is complete and proper baseline flow can be demonstrated with the current airfoil, work can begin to characterize the effectiveness of the two-actuator layout. After demonstrating the control

authority, the system parameters can be optimized. These parameters include the optimal locations for each actuator, the optimal frequency with which to force each actuator, as well as observing the link between these two. If this is completed, an effort can be made to incorporate the system into a more robust feedback controller. Enhancements that can be made to the current algorithm include a method to detect and avoid divergence, as well as possibly investigating the use of multiple sensing techniques in addition or in place of the hot-films.

REFERENCES

Anonymous. *Airfoil.* March 28, 2012. http://en.wikipedia.org/w/index.php?title=Airfoil&action=history (accessed April 28, 2012).

—. *Angle of Attack.* December 13, 2009. http://www.aviation-history.com/theory/angle_of_attack.htm (accessed April 28, 2012).

—. *Plasma (physics).* April 20, 2012. http://en.wikipedia.org/wiki/Plasma_%28physics%29 (accessed April 28, 2012).

Benard, Nicolas, Eric Moreau, John Griffin, and Louis N. Cattafesta III. "Slope seeking for autonomous lift improvement by plasma surface discharge." *Experiments in Fluids* 48 (2010): 791-808.

Corke, Thomas C., Lon C. Enloe, and Stephen P. Wilkinson. "Dielectric Barrier Discharge Plasma Actuators for Flow Control." *Annual Review of Fluid Mechanics* 42 (2010): 505-529.

Devenport, W. J., and W. L. Hartwell. "Experiment 1 - Flow Visualization." December 20, 2006. http://www.dept.aoe.vt.edu/~devenpor/aoe3054/manual/expt1/text.html (accessed April 28, 2012).

Gad-el-Hak, Mohamed, and Dennis M. Bushnell. "Separation Control: Review." *Journal of Fluids Engineering* 113 (March 1991): 5-30.

Greenblatt, David, and Wygnanski J. Israel. "The control of flow separation by periodic excitation." *Progress in Aerospace Sciences* 36 (2000): 487-545.

Houghton, E. L., P. W. Carpenter, Steven H. Collicott, and Daniel T. Valentine. *Aerodynamics for Enineering Students*. Waltham, Massachusetts: Elsevier, 2013.

Jacobs, Eastman N., Kenneth E. Ward, and Robert M. Pinkerton. "The Characteristics of 78 Related Airfoil Sections from Test in the Variable-Density Wind Tunnel." *National Advisory Committee for Aeronautics Report* No. 460 (1935).

Little, Jesse C. "High-Lift Airfoil Separation Control with Dielectric Barrier Discharge Plasma Actuators." Dissertation, Mechanical Engineering, The Ohio State University, Columbus, Ohio, 2010, 217.

Niekamp, Troy S. "Active Flow Separation Control on Wall-Mounted Hump Using NS-Pulsed Dielectric Barrier Discharge Plasma Actuation." Undergraduate Thesis, Mechanical Engineering, The Ohio State University, Columbus, Ohio, 2011, 48.

Rethmel, Christopher, Jesse Little, Takashima, K., A. Sinha, I. Adamovich, and M. Samimy. "Flow Separation Control over an Airfoil with Nanosecond Pulse Driven DBD Plasma Actuators." *49th AIAA Aerspace Sciences Meeting.* Orlando, Florida, 2011.

Roupassov, D. V., A. A. Nikipelov, M. M. Nudnova, and A. Yu. Starikovskii. "Flow Separation Control by Plasma Actuator with Nanosecond Pulsed-Periodic Discharge." *AIAA Journal* 47, no. 1 (January 2009): 168-185.

Seifart, A., A. Darabi, and I. Wygnanski. "Delay of Airfoil Stall by Periodic Excitation." *Journal of Aircraft* 33, no. 4 (July-August 1996): 691-698.

Sinha, A., K. Kim, A. Serrani, and M. Samimy. "Extremizing Feedback Control of a High-Speed and High Reynolds Number Jet." *AIAA Journal* 48, no. 2 (2012): 387-399.

Takashima, Keisuke, Yvette Zuzeek, Walter R. Lempert, and Igor V. Adamovich. "Characterization of a surface dielectric barrier discharge plasma sustained by repetitive nanosecond pulses." *Plasma Sources Science and Technology* 20 (September 2011): 1-10.